



# Seismic stability and failure mode of the slope containing a two-pile foundation

Wenzhe Peng<sup>1,2</sup> · Minghua Zhao<sup>1,2</sup> · Heng Zhao<sup>1,2</sup> · Chaowei Yang<sup>1,2</sup>

Received: 28 April 2022 / Accepted: 9 December 2022 / Published online: 3 January 2023  
© Springer-Verlag GmbH Germany, part of Springer Nature 2023

## Abstract

In this study, the seismic stability of the slope containing a two-pile foundation (SCTPF) under seismic loads is evaluated by the finite element limit analysis (FELA) method. The seismic loading is modeled as a statically applied inertial force, the magnitude of which is a product of a seismic coefficient and the weight of the potential sliding mass within the framework of the pseudo-static method. The feasibility of FELA in the analysis is validated by comparing the predicted safety factors, yield acceleration coefficients, and potential failure surfaces with those in published studies. On this basis, some non-dimensional multipliers are presented to investigate the variations of seismic safety factors with different factors and simplify the calculation of seismic safety factors. Numerous values of the multipliers under different conditions have been given in this study and the tendency of these multipliers with different factors has been explored by fitting curves or distribution regions. Furthermore, four detailed design tables for seismic safety factors and six representative slope failure modes are presented, with the mechanisms and conditions of these failure modes and the transitions among them elaborated.

**Keywords** Slope seismic stability · Laterally loaded pile · Finite element limit analysis · Two-pile foundation · Factor of safety

## Introduction

The pile foundation is the most commonly used foundation for various structures (e.g., road and railway bridges, high-rise buildings, transmission towers, and wind turbine towers) in mountainous areas (Ng and Zhang 2001; Peng et al. 2019), as depicted in Fig. 1a (Peng et al. 2022a). In particular, the two-pile foundation (Fig. 1b), a special pile foundation, is frequently employed to address the considerable internal force

and deformation of piles in these regions such as the central and western mountainous areas in China (Peng et al. 2020). The two-pile foundation would inevitably sustain the lateral loads atop the pile due to the earthquake, vehicle braking, and strong wind (Liang et al. 2012; Zhang et al. 2020, 2021), in addition to axial loads (Dai et al. 2012). The slope stability would degenerate owing to the indirect lateral loads (Ng et al. 2001) transferred from the superstructure (inc. the earthquake-induced inertial force) as well as the direct seismic loads (Joorabchi et al. 2014; Li et al. 2016).

Much more effort has been devoted to the pile behaviors in mountainous areas (Muthukkumaran 2014; Nimityongskul et al. 2018) rather than the effect of piles on surrounding strata, e.g., the slope stability containing laterally loaded piles (Nakasima et al. 1985; Uto et al. 1987). Former studies have mainly focused on the effect of slope on the pile bearing capacity (Peng et al. 2021) and pile deformation characteristics (Jiang et al. 2020). However, numerical observations demonstrated that the slope stability will decrease significantly or even to an unsafe level when the pile foundation in the slope is laterally loaded (Ng et al. 2001). Therefore, the change of slope stability should be equally focused on when designing a pile foundation in mountainous areas. The wedge failure

✉ Heng Zhao  
henrychiu@hnu.edu.cn

Wenzhe Peng  
wzpeng@hnu.edu.cn

Minghua Zhao  
mhzhaohd@21cn.com

Chaowei Yang  
cwyang@hnu.edu.cn

<sup>1</sup> College of Civil Engineering, Hunan University, Changsha 410082, People's Republic of China

<sup>2</sup> Key Laboratory of Building Safety and Energy Efficiency, Ministry of Education, Hunan University, Changsha 410082, People's Republic of China

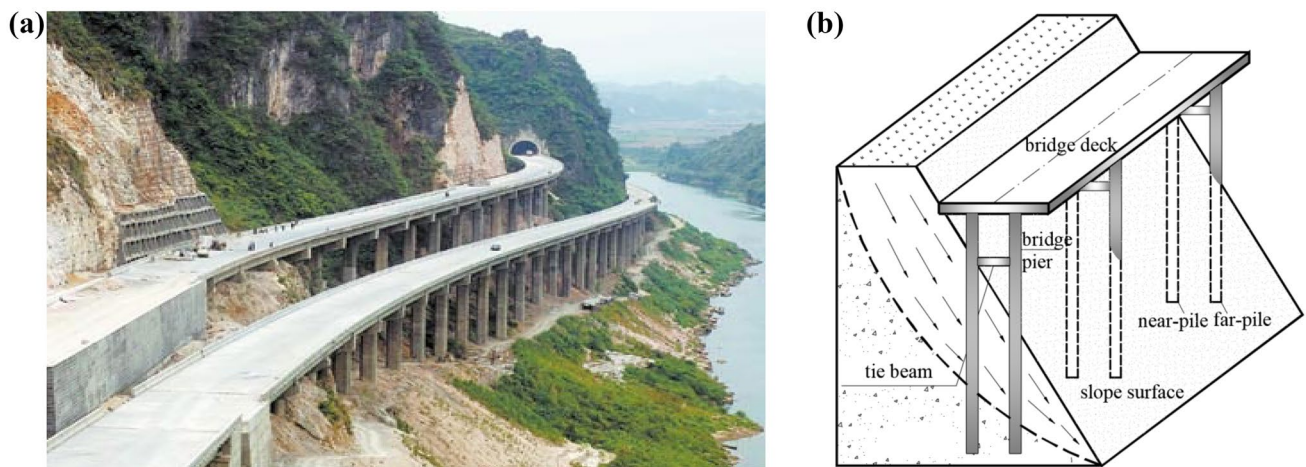


**Fig. 1** Pile foundations in mountainous areas: **a** road bridge in engineering practice (Peng et al. 2022a); **b** two-pile foundations in bridge engineering

in front of laterally loaded piles in sloping ground has been observed by laboratory experiments (Muthukkumaran 2014) and full-scale tests (Nimityongskul et al. 2018). Inspired by these studies, the asymmetric failure mode has been presented to characterize the wedge failure of soil in front of laterally loaded piles in sloping ground (Peng et al. 2021). Another extreme case of seismic load, however, has not been referred to in the aforementioned studies. To meet the requirement for seismic stability of slopes containing bridge pile foundations (JTG 3363–2019, 2020), the effects of seismic loads and laterally loaded single piles on the seismic stability of these slopes have been investigated by the finite element limit analysis method within the framework of the pseudo-static method (Peng et al. 2022b).

As mentioned above, however, the two-pile foundation is frequently used by bridge engineering in mountainous areas and the seismic stability of the slope containing a two-pile foundation (SCTPF) has been rarely mentioned. It can be accepted that the tie beam would significantly affect the internal force and deformation of piles, as well as the lateral loads transferred from the bridge superstructure to the slope (Peng et al. 2020). It can be inferred that there would be obvious distinctions between the seismic stabilities of the slopes containing a two-pile foundation and a laterally loaded single pile. To the authors' knowledge, the structure of the two-pile foundation is similar to that of special anti-slide piles, i.e., portal piles (Zhao et al. 2017) and h-type piles (Xiao et al. 2017; Liu et al. 2018). Hence, there are certain similarities between the seismic stabilities of SCTPF and those reinforced with portal piles or h-type piles.

Recently, the finite element limit analysis (FELA) method (Sloan 2013) has been developed to evaluate the stability of slopes reinforced with anti-slide piles by imposing the finite element method (Liyanapathirana and Poulos 2010) and the limit theorem of plasticity (Gao et al. 2014). In the FELA method (Kumar and Chakraborty 2013), only

the ultimate failure mechanism and corresponding factor of safety would be demonstrated, and the absolute internal force and deformation during the intermediate process would not be obtained. It differs from other conventional methods, e.g., the limit equilibrium method (Poulos 1995; Hassiotis et al. 1997), limit analysis method (Ausilio et al. 2001; Nian et al. 2008; Li et al. 2012), and finite difference method (Ni et al. 2018). As to cases of seismic loading (Lin and Wang 2006; Yan et al. 2020; Huang et al. 2020), the pseudo-static method is widely accepted because of the definite physical significance and simple parameter determination in comparison to Newmark's method and ground response analysis method. Within the framework of the pseudo-static method, the seismic load has been idealized as a seismic acceleration (Loukidis et al. 2003), mainly in the form of the horizontal seismic coefficient in the calculation. On this basis, the slope seismic stability and yield acceleration coefficient have been frequently evaluated by the limit analysis method (Nian et al. 2016) and limit equilibrium method (Joorabchi et al. 2014; Li et al. 2016; Wang et al. 2020). It is also acceptable to adopt the FELA method in the slope seismic stability analysis within the framework of the pseudo-static method. However, the seismic stability of the portal and h-type pile-reinforced slope has been seldom reported, not to mention that of SCTPF.

This study is presented to evaluate the seismic stability of SCTPF by FELA, and the seismic loading has been modeled as a statically applied inertial force, the magnitude of which is a product of a seismic coefficient and the weight of the potential sliding mass. First, the FELA method is successively validated by the cases of a slope containing a laterally loaded single pile (Ng et al. 2001), portal pile-reinforced slope under static conditions (Zhao et al. 2017), and common pile-reinforced slope under seismic conditions (Ausilio et al. 2001; Nian et al. 2016; Li et al. 2016). Subsequently, the effects of various factors (inc. horizontal seismic

coefficient, lateral load atop the pile, slope angle, and shear strength) on the seismic safety factors of SCTPF are further investigated by means of some non-dimensional multipliers. Furthermore, the reasons for the variations of seismic stabilities of SCTPF and the effects of various factors on the failure modes are elaborated. Finally, four design tables for seismic factors of safety are presented to evaluate the seismic stability of SCTPF, and six typical failure modes are concluded.

### Problem definition

Figure 2 demonstrates a slope (slope angle  $\theta$  and slope height  $H$ ) containing a two-pile foundation (pile length  $L$ , pile diameter  $D$ , and length of tie beam  $w$ ) under seismic loads. The effect of groundwater is ignored because the groundwater level is well below the pile tip. The slope consists of  $c$ - $\varphi$  soil (unit weight  $\gamma$ ), whose shear strength is characterized by the cohesion  $c$  and internal friction angle  $\varphi$ . To generalize the results in this study, two normalized parameters are defined as follows: normalized lateral load atop the pile,  $N_Q = Q/Q_u$  ( $Q_u$  denotes the ultimate shear resistance of pile, given by  $Q_u = 0.8f_c^{0.5}D^2$  (BS 8110 1985), thereinto,  $f_c$  symbolizes the concrete compressive strength); normalized cohesion,  $N_c = c/\gamma D$ . Besides, the seismic load is simulated by a horizontal seismic acceleration, characterized by horizontal seismic coefficient  $k_h$ , within the framework of the pseudo-static method.

### FELA modeling

The FELA method is the combination of finite element discretization and limit theorem of plasticity, and it has been extensively adopted in slope stability analysis because of its accuracy and efficiency, such as the released FELA program

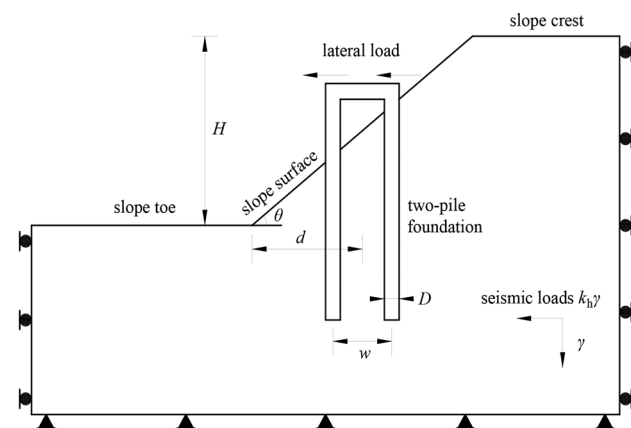


Fig. 2 Problem definition

Optum G2 (Optum Computational Engineering 2017). The method only gives the ultimate failure mechanism and corresponding factor of safety, omitting absolute internal force and deformation during the intermediate process. Employing the FELA method, the upper and lower bound solutions of the slope safety factor can be obtained without presuming the slope failure mechanism.

For this problem, the factor of safety ( $FoS$ ) of the SCTPF under seismic loads can be given as Eq. (1).

$$FoS = f(k_h, N_Q, \theta, \varphi, N_c, H, w, d) \tag{1}$$

The horizontal seismic coefficients are considered as  $k_h = 0, 0.1, 0.2,$  and  $0.3$  (Cinicioglu and Erkli 2018). The normalized lateral loads atop the pile foundation are considered as  $N_Q = 0, 0.03, 0.06, 0.09,$  and  $0.12$  (Ng and Zhang 2001; Ng et al. 2001). The slope angles frequently encountered in bridge engineering in mountainous areas are considered as  $\theta = 20^\circ, 30^\circ, 40^\circ,$  and  $50^\circ$  (Peng et al. 2020, 2022b). The internal friction angles are selected as  $\varphi = 15^\circ, 20^\circ, 25^\circ, 30^\circ,$  and  $35^\circ$ , and the normalized cohesions are selected as  $0.25, 0.5, 0.75,$  and  $1$ , covering most engineering cases. Since the two-pile foundation is generally located in a high slope, whose slope height is greater than 20 m, the slope height  $H = 15D$  and pile diameter  $D = 2$  m are considered. The length of the tie beam adopted in this study is four times the pile diameter, which is usually observed in engineering practice (Peng et al. 2020). In addition, the two-pile foundation is generally constructed at the middle of the slope, similar to the laterally loaded single pile in mountainous areas (Ng et al. 2001; Peng et al. 2022b). Besides these major factors, other secondary factors are set frequently encountered values in engineering practice and the same as those given in Ng et al. (2001), including Young’s modulus, Poisson’s ratios, and unit weight. Hence, the  $FoS$  of SCTPF under seismic loads can be simplified as Eq. (2).

$$FoS = f(k_h, N_Q, \theta, \varphi, N_c) \tag{2}$$

To model the SCTPF under seismic loads, the standard boundary condition is adopted (Peng et al. 2022b), and the soil and pile are simulated by the Mohr–Coulomb material and linear elastic material, respectively. To avoid the boundary effect, the size of the calculation domain was large enough to include all the plastic zones at failure. In this modeling, the length and height of the overall domain are about  $40D$  and  $30D$ , respectively (Fig. 3). The adaptive remeshing technique is adopted in the setting. On this basis, after trials of total elements for a compromise between reducing the error and promoting calculation efficiency, five thousand elements and three iterations of adaptive mesh refinements were adopted throughout the numerical simulations. The delicate setting of the meshing scheme and adaptive mesh refinements can in turn narrow

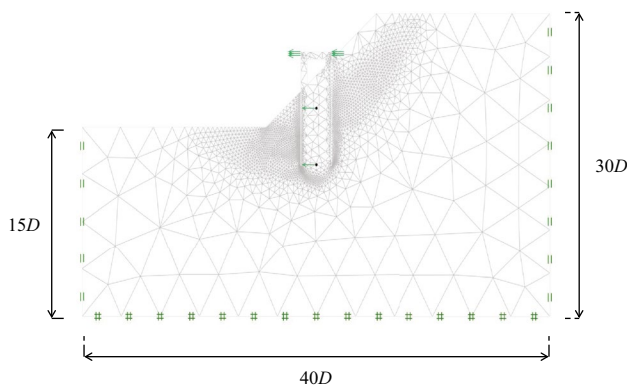


Fig. 3 Numerical modeling of SCTPF under seismic loads

the bounds of the exact collapse load with an error of less than 3%. The worst-case error  $Err$  can be defined based on the upper (UB) and lower bound (LB) solution for the pile bearing capacity,  $Err = \pm 100\% \times 2(UB - LB) / (UB + LB)$ .

### Comparisons with previous studies

There is no proper example case that can be exactly adopted for direct validation of the application of the FELA method in the analysis of the seismic stability of SCTPF. Consequently, only a stepwise validation can be accomplished by three types of degenerated cases: (i) static loading case with a laterally loaded single pile (Ng et al. 2001); (ii) static loading case with portal piles (or h-type piles) (Zhao et al. 2017); and (iii) seismic loading cases with and without anti-slide piles (Ausilio et al. 2001; Nian et al. 2016; Li et al. 2016). Undoubtedly, shear strength parameters were varied in these three recorded cases. The Mohr–Coulomb model, frequently used in the analysis of slope stability problems, is also adopted in this study because of its simplicity for practical use.

### Static conditions

**Case I** The laterally loaded single pile (pile length  $L = 30$  m, embedment depth  $L_{emb} = 22.5$  m) is constructed at the middle of the slope ( $\theta = 32^\circ$  and  $H = 15$  m) composed of completely decomposed granite, and the physical and mechanical parameters of the soil and pile are listed in Table 1. The length and diameter of the pile are 30 m and 2 m, respectively, and the lateral loads atop the pile are considered as  $N_Q = 0, 0.03, 0.06, 0.09, 0.12,$  and  $0.36$  (the normalized design lateral load in engineering practice is  $N_Q = 0.12$ ). The factors of safety of this slope under different lateral loads evaluated from different methods are compared in Fig. 4. It should be supplemented that the slope for the case  $N_Q = 0.36$  is unstable and the corresponding safety factor was not given

Table 1 Physical and mechanical parameters of the soil and pile

Object	Physical and mechanical parameters				
	Young's modulus (MPa)	Poisson's ratio	Unit weight ( $\text{kN/m}^3$ )	Internal friction angle (degree)	Cohesion (kPa)
Soil	50	0.3	18	35	10
Pile	26,000	0.2	24	–	–

by Ng et al. (2001), hence, it has been considered as a value less than 1.0. It can be seen that the factors of safety from FELA coincide well with those given in Ng et al. (2001), indicating that the FELA method can well evaluate the stability of the slope containing a laterally loaded single pile. It can be also observed that the slope stability for the case with piles would be greater than that without piles before the lateral load is applied on the pile head because the pile foundation would provide resistance to some extent. Besides, the safety factors would decrease from 2.07 to 1.86, 1.36, 1.22, and 0.76 while  $N_Q$  increases from 0 to 0.03, 0.06, 0.12, and 0.36, respectively.

**Case II** The Shibagou landslide (about  $\theta = 20^\circ$ ) mainly consists of silty clay, the mechanical parameters of which are not given in the literature (Zhao et al. 2017) and can be empirically given based on the code (GB/T 2021) and handbooks (Editorial Board of Geological Engineering Handbook 2018) about soil classification:  $\phi = 18^\circ, c = 20$  kPa, and the unit weight of soil  $\gamma = 20$   $\text{kN/m}^3$ . To resist the landslide, three kinds of anti-slide piles are suggested to improve slope stability, and their geometry and mechanical parameters can be found in Zhao et al. (2017). The safety factors of different

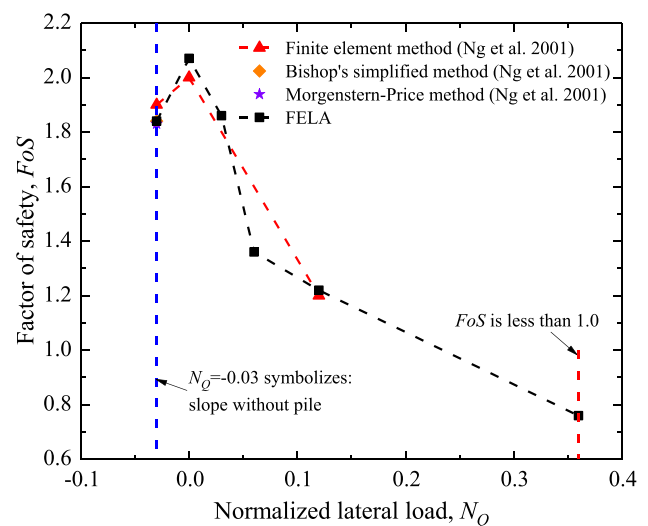


Fig. 4 Safety factors of the slope containing a laterally loaded single pile



anti-slide pile-reinforced slopes are evaluated by different methods and compared in Table 2. As listed in Table 2, the safety factors of the slope evaluated by FELA are 1.24 (portal piles), 1.22 (h-type piles), and 1.11 (common piles), respectively, consistent with those in Zhao et al. (2017). It seems that the FELA can well predict the stability of slopes reinforced with different anti-slide piles, including the portal piles and h-type piles.

### Seismic conditions

**Case III** The typical example slope ( $\theta=30^\circ$  and  $H=13.7$  m) consists of homogeneous materials ( $\varphi=10^\circ$  and  $c=23.94$  kPa), and the soil type is not given in Hassiotis et al. (1997). The static factor of safety for this slope evaluated by FELA is 1.11, which is in good agreement with those of 1.108, 1.11, and 1.134 estimated by the limit analysis method, LAM (Ausilio et al. 2001; Nian et al. 2016) and finite element method, FEM (Nian et al. 2016). As to the seismic factors of safety under seismic conditions ( $k_h=0.05, 0.1, 0.2,$  and  $0.3$ ), the predictions from different methods are presented in Table 3.

Since the factors of safety in Table 3 are on the unsafe side, the anti-slide piles are placed in the slope, and the distance between the pile and slope toe is  $d=12.2$  m. To investigate the effect of anti-slide piles on the safety factor, a yield acceleration coefficient  $k_y$  is proposed to define the acceleration coefficient when the factor of safety equals 1.0 (Joorabchi et al. 2014; Li et al. 2016). Besides the case ( $\varphi=10^\circ$  and  $c=23.94$  kPa), other two sets of shear strength parameters ( $\varphi=15^\circ$  and  $c=23.94$  kPa;  $\varphi=15^\circ$  and  $c=18$  kPa) are used for the extended discussion of the yield acceleration coefficient. The yield acceleration coefficients of these cases from different methods such as the limit equilibrium method (LEM), LAM, and FELA are compared in Table 4.

Tables 3 and 4 indicate that the predictions (factors of safety and yield acceleration coefficients) in this study coincide well with those from published studies. Furthermore, Fig. 5 reveals that the potential failure surfaces under different seismic conditions ( $k_h=0.049$ , without piles;  $k_h=0.1$ , without piles;  $k_h=0.2$ , with piles) given by FELA are well consistent with those estimated by Li et al. (2016) and Nian et al. (2016), still only dealing with the case with  $\varphi=10^\circ$  and  $c=23.94$  kPa. To sum up, these aforementioned comparisons

**Table 2** Comparisons between safety factors of pile-reinforced slopes

Pile types	Factor of safety	
	Zhao et al. (2017)	FELA
Portal piles	1.22	1.24
h-type piles	1.21	1.22
Common piles	1.09	1.11

**Table 3** Comparisons of safety factors

Horizontal seismic coefficient $k_h$	Factors of safety ( $FoS$ )			
	LAM		FEM (Nian et al. 2016)	FELA
	Ausilio et al. (2001)	Nian et al. (2016)		
0	1.108	1.11	1.134	1.11
0.05	–	1.00	1.017	0.997
0.1	–	0.91	0.918	0.907
0.2	–	0.75	0.761	0.756
0.3	–	0.64	0.643	0.639

indicate that the FELA can be employed to evaluate seismic factors of safety, yield acceleration coefficients, and potential failure surfaces of slopes reinforced with piles.

## Results and discussions

The effects of various factors on the seismic stability of SCTPF would be investigated in terms of the following aspects, including the horizontal seismic coefficient  $k_h$ , normalized lateral load atop the pile  $N_Q$ , slope angle  $\theta$ , internal friction angle  $\varphi$ , and normalized cohesion  $N_c$ . Utilizing the FELA method, four detailed design tables for the seismic safety factors of SCTPF are presented in Tables 5, 6, 7, and 8. Furthermore, some non-dimensional multipliers are proposed for general application, including the multiplier of seismic coefficient  $\xi_k$ , the multiplier of lateral load  $\xi_Q$ , the multiplier of slope angle  $\xi_\theta$ , the multiplier of internal friction angle  $\xi_\varphi$ , and the multiplier of cohesion  $\xi_c$ , which are defined as Eqs. (3) to (7).

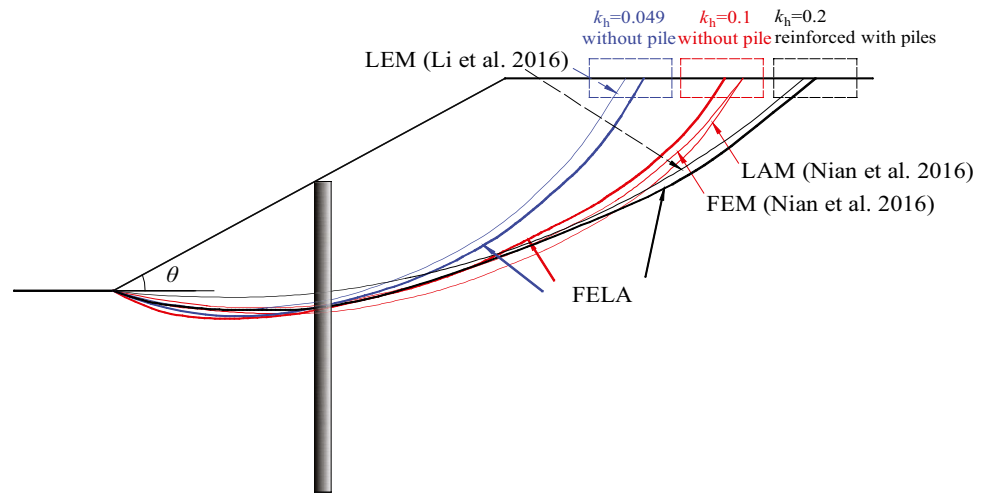
$$\xi_k = \frac{FoS(k_h)}{FoS(k_h = 0)} \tag{3}$$

$$\xi_Q = \frac{FoS(N_Q)}{FoS(N_Q = 0)} \tag{4}$$

**Table 4** Comparisons between yield acceleration coefficients from different methods

$\varphi$ (degree)	$c$ (kPa)	Yield acceleration coefficient $k_y$			
		LEM	LAM		FELA
		Joorabchi et al. (2014)	Li et al. (2016)	(Li et al. 2010)	
10	23.94	0.23	0.25	0.25	0.29
15	23.94	0.34	0.35	0.35	0.38
15	18	0.28	0.27	0.27	0.30

**Fig. 5** Potential failure surfaces under different seismic conditions



$$\xi_{\theta} = \frac{FoS(\theta)}{FoS(\theta = 20^{\circ})} \tag{5}$$

$$\xi_{\varphi} = \frac{FoS(\varphi)}{FoS(\varphi = 15^{\circ})} \tag{6}$$

$$\xi_{N_c} = \frac{FoS(N_c)}{FoS(N_c = 0.25)} \tag{7}$$

These non-dimensional multipliers are presented to reveal the variations of seismic safety factors of SCTPF and simplify the prediction of the seismic safety factors. For example, the seismic safety factor,  $FoS(k_h)$ , is the product of the static safety factor,  $FoS(k_h=0)$ , and the corresponding multiplier of the seismic coefficient,  $\xi_k$ . These multipliers have been seldom mentioned but are believed to be useful for the preliminary design of engineering practice.

**Horizontal seismic coefficient**

Figure 6 illustrates the variations of the multiplier of seismic coefficient,  $\xi_k$ , with  $k_h$  under different slope angles and lateral loads, and four groups of representative shear strength parameters ( $\varphi = 20^{\circ}, N_c = 0.25$ ;  $\varphi = 25^{\circ}, N_c = 0.5$ ;  $\varphi = 30^{\circ}, N_c = 0.75$ ;  $\varphi = 35^{\circ}, N_c = 1$ ) are taken into consideration. As anticipated, the multiplier of the seismic coefficient nonlinearly decreases with  $k_h$ , and so does the seismic safety factor of SCTPF. Furthermore, the variations of  $\xi_k$  with  $k_h$  can be fitted by quadratic functions,  $\xi_k = 1 - B_{k,1} \cdot k_h + B_{k,2} \cdot k_h^2$  (Fig. 6). In addition, the multiplier of the seismic coefficient is positively correlated with  $\theta$  and  $N_Q$ , revealing that the effect of seismic loads on the slope seismic stability would be weakened with the increase of  $\theta$  and  $N_Q$ . It can be observed that the multiplier of the seismic coefficient,

which mainly depends on  $k_h, \theta$ , and  $N_Q$ , is not sensitive to shear strength, hence the FELA results and corresponding fitting curves (Fig. 6) can be generalized to cases of other shear strengths.

Figure 7 demonstrates the plastic multipliers of an example SCTPF ( $\theta = 30^{\circ}$  and  $N_Q = 0.06$ ) under different horizontal seismic coefficients ( $k_h = 0, 0.1, 0.2$ , and  $0.3$ ). The shear strength parameters of  $\varphi = 25^{\circ}$  and  $N_c = 0.5$  are selected as the representative shear strength parameters considering that the multiplier of the seismic coefficient is not sensitive to shear strength. The different magnitudes of plastic multiplier are characterized by different colors, and the variation of the color from blue to red indicates the increase of plastic multiplier. It should be pointed out that the specific color does not represent an absolute value of plastic multiplier. However, the relative magnitudes of plastic multipliers can be reflected by the color contrast, and the potential failure surface can be outlined. A clear potential failure surface from the slope crest to the slope toe can be observed while  $k_h > 0.1$ , but it would not occur at  $k_h = 0$ . Besides, the tension failure behind the pile foundation, resulting from the difference between the deformations of the pile and slope, would be more obvious and move closer to the slope crest with the increase of the horizontal seismic coefficient.

**Lateral load**

Figure 8 draws the variations of the multiplier of lateral load,  $\xi_Q$ , with  $N_Q$  under different horizontal seismic coefficients and slope angles, and four groups of representative shear strength parameters ( $\varphi = 20^{\circ}, N_c = 0.25$ ;  $\varphi = 25^{\circ}, N_c = 0.5$ ;  $\varphi = 30^{\circ}, N_c = 0.75$ ;  $\varphi = 35^{\circ}, N_c = 1$ ) are taken into consideration. As expected, the multiplier of lateral load nonlinearly decreases with  $N_Q$ , and so does the seismic safety factor

**Table 5** Factors of safety ( $\theta=20^\circ$ )

$k_h$	$N_Q$	$\varphi$	$N_c$				$N_Q$	$\varphi$	$N_c$				
			0.25	0.5	0.75	1			0.25	0.5	0.75	1	
0	0.03	15	0.97	1.11	1.25	1.39	0.06	15	0.79	0.92	1.04	1.17	
		20	1.26	1.40	1.54	1.69		20	1.02	1.15	1.28	1.41	
		25	1.57	1.72	1.87	2.02		25	1.28	1.41	1.53	1.66	
		30	1.90	2.05	2.21	2.37		30	1.55	1.68	1.81	1.94	
		35	2.28	2.43	2.59	2.75		35	1.85	1.98	2.11	2.24	
	0.09	15	0.65	0.76	0.86	0.97	0.12	15	0.55	0.64	0.72	0.81	
		20	0.85	0.96	1.06	1.17		20	0.72	0.81	0.89	0.98	
		25	1.06	1.16	1.27	1.37		25	0.90	0.99	1.07	1.16	
		30	1.28	1.39	1.49	1.60		30	1.10	1.18	1.27	1.35	
		35	1.54	1.64	1.75	1.85		35	1.31	1.39	1.48	1.56	
	0.1	0.03	15	0.76	0.87	0.97	1.08	0.06	15	0.65	0.75	0.86	0.96
			20	1.00	1.11	1.21	1.32		20	0.85	0.95	1.06	1.16
			25	1.24	1.35	1.47	1.58		25	1.06	1.16	1.27	1.37
			30	1.50	1.62	1.73	1.85		30	1.29	1.40	1.50	1.61
			35	1.80	1.92	2.04	2.16		35	1.54	1.64	1.75	1.85
0.09		15	0.56	0.65	0.74	0.83	0.12	15	0.49	0.57	0.64	0.72	
		20	0.73	0.82	0.91	1.00		20	0.65	0.72	0.80	0.87	
		25	0.92	1.01	1.09	1.18		25	0.81	0.88	0.96	1.03	
		30	1.11	1.20	1.29	1.38		30	0.99	1.06	1.13	1.20	
		35	1.33	1.42	1.51	1.60		35	1.18	1.25	1.33	1.40	
0.2		0.03	15	0.63	0.71	0.80	0.88	0.06	15	0.55	0.63	0.72	0.80
			20	0.82	0.91	0.99	1.08		20	0.72	0.81	0.89	0.98
			25	1.02	1.11	1.20	1.29		25	0.90	0.99	1.08	1.17
			30	1.24	1.33	1.42	1.51		30	1.10	1.19	1.27	1.36
			35	1.48	1.57	1.67	1.76		35	1.31	1.40	1.49	1.58
	0.09	15	0.50	0.57	0.65	0.72	0.12	15	0.45	0.51	0.58	0.64	
		20	0.65	0.72	0.80	0.87		20	0.58	0.65	0.71	0.78	
		25	0.81	0.88	0.96	1.03		25	0.73	0.80	0.86	0.93	
		30	0.98	1.06	1.13	1.21		30	0.89	0.95	1.02	1.08	
		35	1.17	1.25	1.32	1.40		35	1.07	1.13	1.20	1.26	
	0.3	0.03	15	0.52	0.59	0.67	0.74	0.06	15	0.48	0.55	0.61	0.68
			20	0.69	0.76	0.84	0.91		20	0.63	0.70	0.77	0.84
			25	0.86	0.93	1.01	1.08		25	0.79	0.86	0.93	1.00
			30	1.05	1.12	1.20	1.27		30	0.95	1.03	1.10	1.18
			35	1.25	1.33	1.41	1.49		35	1.14	1.22	1.29	1.37
0.09		15	0.44	0.50	0.57	0.63	0.12	15	0.40	0.46	0.52	0.58	
		20	0.57	0.64	0.70	0.77		20	0.53	0.59	0.64	0.70	
		25	0.72	0.79	0.85	0.92		25	0.66	0.72	0.78	0.84	
		30	0.87	0.94	1.00	1.07		30	0.80	0.86	0.93	0.99	
		35	1.05	1.12	1.18	1.25		35	0.96	1.02	1.08	1.14	

of SCTPF. Furthermore, the variations of  $\xi_Q$  with  $N_Q$  can be fitted by quadratic functions,  $\xi_Q = 1 - B_{Q,1} \cdot N_Q + B_{Q,2} \cdot N_Q^2$  (Fig. 8). In addition, the multiplier of lateral load is positively correlated with  $k_h$  and negatively correlated with  $\theta$ , indicating that the effect of  $N_Q$  on the slope seismic stability would be weakened with  $k_h$  but enhanced with  $\theta$ . Furthermore, the effect of lateral loads on the seismic slope stability cannot be neglected even in the cases  $k_h=0.3$ , revealing

that the lateral load should be considered in the design of bridge pile foundation engineering. It can be observed that the multiplier of lateral load, which mainly depends on  $N_Q$ ,  $k_h$ , and  $\theta$ , is hardly ever affected by the shear strength, hence the FELA results and corresponding fitting curves (Fig. 8) can be generalized to cases of other shear strengths.

Figure 9 gives the plastic multipliers of an example SCTPF ( $\theta = 40^\circ$ ,  $k_h = 0.2$ ,  $\varphi = 25^\circ$ , and  $N_c = 0.5$ ) under

**Table 6** Factors of safety ( $\theta=30^\circ$ )

$k_h$	$N_Q$	$\varphi$	$N_c$				$N_Q$	$\varphi$	$N_c$				
			0.25	0.5	0.75	1			0.25	0.5	0.75	1	
0	0.03	15	0.75	0.87	1.00	1.12	0.06	15	0.61	0.71	0.82	0.92	
		20	0.97	1.10	1.22	1.35		20	0.79	0.90	1.00	1.11	
		25	1.21	1.34	1.46	1.59		25	0.98	1.09	1.19	1.30	
		30	1.46	1.59	1.72	1.85		30	1.19	1.30	1.40	1.51	
		35	1.75	1.88	2.01	2.14		35	1.43	1.53	1.64	1.74	
	0.09	15	0.51	0.60	0.68	0.77	0.12	15	0.44	0.51	0.58	0.65	
		20	0.66	0.75	0.83	0.92		20	0.58	0.65	0.71	0.78	
		25	0.83	0.91	1.00	1.08		25	0.72	0.79	0.85	0.92	
		30	1.00	1.09	1.17	1.26		30	0.88	0.95	1.01	1.08	
		35	1.20	1.29	1.37	1.46		35	1.05	1.12	1.18	1.25	
	0.1	0.03	15	0.63	0.73	0.82	0.92	0.06	15	0.53	0.62	0.71	0.80
			20	0.81	0.91	1.02	1.12		20	0.69	0.78	0.87	0.96
			25	1.01	1.12	1.22	1.33		25	0.86	0.95	1.04	1.13
			30	1.23	1.34	1.44	1.55		30	1.04	1.13	1.22	1.31
			35	1.47	1.58	1.69	1.80		35	1.25	1.34	1.43	1.52
0.09		15	0.46	0.53	0.61	0.68	0.12	15	0.40	0.46	0.53	0.59	
		20	0.60	0.67	0.75	0.82		20	0.53	0.59	0.65	0.71	
		25	0.75	0.82	0.90	0.97		25	0.66	0.72	0.79	0.85	
		30	0.91	0.98	1.06	1.13		30	0.81	0.87	0.93	0.99	
		35	1.08	1.16	1.23	1.31		35	0.96	1.02	1.09	1.15	
0.2	0.03	15	0.54	0.62	0.70	0.78	0.06	15	0.47	0.55	0.62	0.70	
		20	0.70	0.78	0.87	0.95		20	0.61	0.69	0.76	0.84	
		25	0.87	0.96	1.04	1.13		25	0.76	0.84	0.91	0.99	
		30	1.05	1.14	1.23	1.32		30	0.93	1.01	1.08	1.16	
		35	1.25	1.35	1.44	1.54		35	1.10	1.18	1.26	1.34	
	0.09	15	0.42	0.48	0.55	0.61	0.12	15	0.37	0.43	0.48	0.54	
		20	0.54	0.61	0.67	0.74		20	0.49	0.55	0.60	0.66	
		25	0.68	0.74	0.81	0.87		25	0.61	0.67	0.72	0.78	
		30	0.82	0.89	0.95	1.02		30	0.75	0.80	0.86	0.91	
		35	0.98	1.05	1.12	1.19		35	0.89	0.95	1.00	1.06	
0.3	0.03	15	0.47	0.54	0.60	0.67	0.06	15	0.42	0.48	0.55	0.61	
		20	0.61	0.68	0.75	0.82		20	0.55	0.62	0.68	0.75	
		25	0.76	0.83	0.91	0.98		25	0.68	0.75	0.81	0.88	
		30	0.92	1.00	1.07	1.15		30	0.83	0.90	0.96	1.03	
		35	1.09	1.17	1.25	1.33		35	0.99	1.06	1.13	1.20	
	0.09	15	0.38	0.44	0.50	0.56	0.12	15	0.35	0.40	0.45	0.50	
		20	0.50	0.56	0.61	0.67		20	0.45	0.50	0.56	0.61	
		25	0.62	0.68	0.74	0.80		25	0.57	0.62	0.68	0.73	
		30	0.75	0.81	0.87	0.93		30	0.69	0.74	0.80	0.85	
		35	0.90	0.96	1.02	1.08		35	0.83	0.88	0.94	0.99	

different lateral loads ( $N_Q=0, 0.03, 0.06, 0.09,$  and  $0.12$ ). Some differences can be observed between the failure modes of SCTPF ( $N_Q=0.03, 0.06, 0.09,$  and  $0.12$ ) and portal pile-reinforced slopes ( $N_Q=0$ ); for the former, the slope failure mainly results from the tension failure behind the pile foundation (Fig. 9b to d), whereas a clear potential failure surface from the slope crest to the slope toe occurs in the latter (Fig. 9a). To sum up, the effect of lateral load

on the seismic stability and failure mode of SCTPF cannot be ignored in engineering practice.

**Slope angle**

Figure 10 illustrates the variations of the multiplier of slope angle,  $\xi_\theta$ , with  $\theta$  under different horizontal seismic coefficients and lateral loads, and four groups of representative



**Table 7** Factors of safety ( $\theta=40^\circ$ )

$k_h$	$N_Q$	$\varphi$	$N_c$				$N_Q$	$\varphi$	$N_c$				
			0.25	0.5	0.75	1			0.25	0.5	0.75	1	
0	0.03	15	0.64	0.75	0.86	0.97	0.06	15	0.52	0.61	0.70	0.79	
		20	0.83	0.94	1.05	1.16		20	0.67	0.76	0.86	0.95	
		25	1.03	1.14	1.26	1.37		25	0.83	0.92	1.02	1.11	
		30	1.24	1.36	1.47	1.59		30	1.01	1.10	1.20	1.29	
		35	1.45	1.58	1.71	1.84		35	1.21	1.30	1.40	1.49	
	0.09	15	0.43	0.51	0.58	0.66	0.12	15	0.38	0.44	0.50	0.56	
		20	0.57	0.64	0.72	0.79		20	0.49	0.55	0.61	0.67	
		25	0.71	0.78	0.85	0.92		25	0.62	0.68	0.73	0.79	
		30	0.86	0.93	1.00	1.07		30	0.75	0.81	0.87	0.93	
		35	1.03	1.10	1.17	1.24		35	0.90	0.96	1.01	1.07	
	0.1	0.03	15	0.55	0.64	0.74	0.83	0.06	15	0.46	0.54	0.62	0.70
			20	0.71	0.81	0.90	1.00		20	0.60	0.68	0.76	0.84
			25	0.89	0.98	1.08	1.17		25	0.75	0.83	0.91	0.99
			30	1.08	1.18	1.27	1.37		30	0.91	0.99	1.07	1.15
			35	1.23	1.35	1.46	1.58		35	1.09	1.17	1.25	1.33
0.09		15	0.40	0.47	0.53	0.60	0.12	15	0.35	0.41	0.46	0.52	
		20	0.52	0.58	0.65	0.71		20	0.46	0.51	0.57	0.62	
		25	0.65	0.71	0.78	0.84		25	0.58	0.63	0.69	0.74	
		30	0.80	0.86	0.93	0.99		30	0.71	0.76	0.81	0.86	
		35	0.95	1.01	1.08	1.14		35	0.85	0.90	0.96	1.01	
0.2		0.03	15	0.48	0.56	0.64	0.72	0.06	15	0.42	0.49	0.55	0.62
			20	0.63	0.71	0.79	0.87		20	0.55	0.62	0.68	0.75
			25	0.78	0.86	0.95	1.03		25	0.68	0.75	0.82	0.89
			30	0.92	1.01	1.10	1.19		30	0.82	0.89	0.96	1.03
			35	1.06	1.17	1.27	1.38		35	0.99	1.06	1.13	1.20
	0.09	15	0.37	0.43	0.49	0.55	0.12	15	0.33	0.38	0.43	0.48	
		20	0.48	0.54	0.60	0.66		20	0.44	0.49	0.53	0.58	
		25	0.60	0.66	0.72	0.78		25	0.55	0.60	0.64	0.69	
		30	0.73	0.79	0.85	0.91		30	0.67	0.72	0.76	0.81	
		35	0.88	0.94	1.00	1.06		35	0.80	0.85	0.90	0.95	
	0.3	0.03	15	0.43	0.50	0.56	0.63	0.06	15	0.38	0.44	0.50	0.56
			20	0.56	0.63	0.69	0.76		20	0.50	0.56	0.62	0.68
			25	0.69	0.76	0.84	0.91		25	0.62	0.68	0.75	0.81
			30	0.80	0.89	0.97	1.06		30	0.75	0.81	0.88	0.94
			35	0.92	1.02	1.13	1.23		35	0.89	0.96	1.02	1.09
0.09		15	0.34	0.39	0.45	0.50	0.12	15	0.31	0.36	0.40	0.45	
		20	0.45	0.50	0.56	0.61		20	0.41	0.46	0.50	0.55	
		25	0.56	0.61	0.67	0.72		25	0.52	0.56	0.61	0.65	
		30	0.68	0.73	0.79	0.84		30	0.62	0.67	0.72	0.77	
		35	0.81	0.87	0.92	0.98		35	0.75	0.80	0.84	0.89	

shear strength parameters ( $\varphi = 20^\circ, N_c = 0.25; \varphi = 25^\circ, N_c = 0.5; \varphi = 30^\circ, N_c = 0.75; \varphi = 35^\circ, N_c = 1$ ) are taken into consideration. It can be seen that the multiplier of slope angle linearly decreases with  $\theta$ , and so does the seismic safety factor of SCTPF. Furthermore, the variations of  $\xi_\theta$  with  $\theta$  can be fitted by linear functions,  $\xi_\theta = B_{\theta,1} \cdot \theta + B_{\theta,2}$

(Fig. 10). The fitted coefficients  $B_{\theta,1}$  (the slope of the fitted curve) under different horizontal seismic coefficients are equal and vary slightly with  $N_Q$ , while the fitted coefficients  $B_{\theta,2}$  (intercept of the fitted curve) increase with  $k_h$  and also vary slightly with  $N_Q$ . In addition, keeping all other factors the same, the multiplier of slope angle seems to have little

**Table 8** Factors of safety ( $\theta=50^\circ$ )

$k_h$	$N_Q$	$\varphi$	$N_c$				$N_Q$	$\varphi$	$N_c$				
			0.25	0.5	0.75	1			0.25	0.5	0.75	1	
0	0.03	15	0.54	0.64	0.75	0.85	0.06	15	0.42	0.50	0.59	0.67	
		20	0.69	0.80	0.90	1.01		20	0.54	0.62	0.71	0.79	
		25	0.86	0.97	1.07	1.18		25	0.67	0.75	0.84	0.92	
		30	1.04	1.15	1.25	1.36		30	0.82	0.90	0.98	1.06	
		35	1.23	1.34	1.45	1.56		35	0.98	1.06	1.14	1.22	
	0.09	15	0.35	0.41	0.48	0.54	0.12	15	0.30	0.35	0.40	0.45	
		20	0.45	0.51	0.58	0.64		20	0.40	0.45	0.49	0.54	
		25	0.57	0.63	0.69	0.75		25	0.50	0.54	0.59	0.63	
		30	0.69	0.75	0.81	0.87		30	0.61	0.65	0.70	0.74	
		35	0.82	0.88	0.94	1.00		35	0.73	0.77	0.82	0.86	
	0.1	0.03	15	0.47	0.56	0.64	0.73	0.06	15	0.38	0.45	0.53	0.60
			20	0.61	0.70	0.79	0.88		20	0.49	0.56	0.64	0.71
			25	0.75	0.84	0.94	1.03		25	0.62	0.69	0.76	0.83
			30	0.91	1.00	1.10	1.19		30	0.75	0.82	0.89	0.96
			35	1.08	1.17	1.27	1.36		35	0.89	0.96	1.04	1.11
0.09		15	0.33	0.39	0.44	0.50	0.12	15	0.29	0.33	0.38	0.42	
		20	0.42	0.48	0.53	0.59		20	0.38	0.42	0.47	0.51	
		25	0.53	0.58	0.64	0.69		25	0.47	0.51	0.56	0.60	
		30	0.65	0.70	0.76	0.81		30	0.58	0.62	0.66	0.70	
		35	0.77	0.82	0.88	0.93		35	0.70	0.74	0.78	0.82	
0.2		0.03	15	0.42	0.49	0.57	0.64	0.06	15	0.35	0.41	0.48	0.54
			20	0.54	0.62	0.69	0.77		20	0.46	0.52	0.59	0.65
			25	0.67	0.75	0.83	0.91		25	0.56	0.63	0.69	0.76
			30	0.81	0.89	0.97	1.05		30	0.69	0.75	0.82	0.88
			35	0.97	1.05	1.13	1.21		35	0.82	0.88	0.95	1.01
	0.09	15	0.31	0.36	0.41	0.46	0.12	15	0.28	0.32	0.36	0.40	
		20	0.40	0.45	0.50	0.55		20	0.36	0.40	0.44	0.48	
		25	0.50	0.55	0.60	0.65		25	0.45	0.49	0.53	0.57	
		30	0.61	0.66	0.70	0.75		30	0.55	0.59	0.63	0.67	
		35	0.72	0.77	0.82	0.87		35	0.66	0.70	0.74	0.78	
	0.3	0.03	15	0.37	0.44	0.50	0.57	0.06	15	0.32	0.38	0.43	0.49
			20	0.48	0.55	0.61	0.68		20	0.42	0.48	0.53	0.59
			25	0.60	0.67	0.74	0.81		25	0.52	0.58	0.63	0.69
			30	0.73	0.80	0.87	0.94		30	0.63	0.69	0.75	0.81
			35	0.87	0.94	1.01	1.08		35	0.76	0.82	0.88	0.94
0.09		15	0.29	0.34	0.38	0.43	0.12	15	0.26	0.30	0.34	0.38	
		20	0.38	0.43	0.47	0.52		20	0.34	0.38	0.41	0.45	
		25	0.47	0.52	0.56	0.61		25	0.43	0.47	0.50	0.54	
		30	0.57	0.62	0.66	0.71		30	0.52	0.56	0.60	0.64	
		35	0.68	0.73	0.77	0.82		35	0.63	0.67	0.70	0.74	

change with shear strengths. To sum up, the lateral load and shear strength have less influence on the multiplier of slope angle, in comparison to the slope angle and horizontal seismic coefficient.

Figure 11 demonstrates the plastic multipliers of an example SCTPF ( $N_Q=0.06$ ,  $k_h=0.2$ ,  $\varphi=25^\circ$ , and  $N_c=0.5$ ) under different slope angles ( $\theta=20^\circ$ ,  $30^\circ$ ,  $40^\circ$ , and  $50^\circ$ ). Some

distinct differences can be observed between the failure modes of steep slopes ( $\theta=40^\circ$  and  $\theta=50^\circ$ ) and gentle slopes ( $\theta=20^\circ$  and  $\theta=30^\circ$ ); for the former, the slope failure mainly results from the tension failure behind the pile foundation (Fig. 11c and d), but a clear potential failure surface from the slope crest to the slope toe occurs in the latter (Fig. 11a and b).

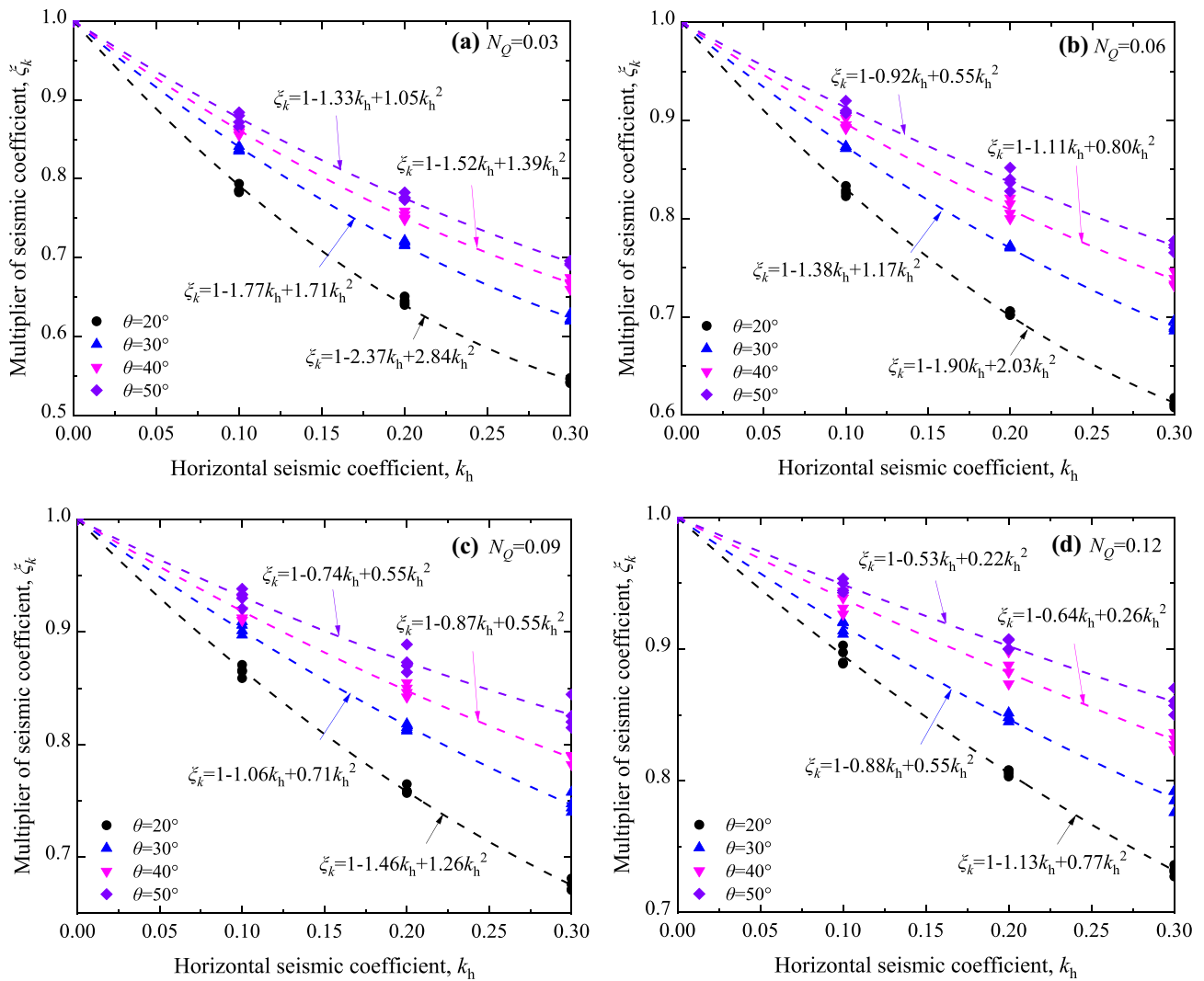


Fig. 6 Variations of  $\xi_k$  under different slope angles

**Internal friction angle and cohesion**

Figure 12 depicts the variations of the multiplier of internal friction angle,  $\xi_\varphi$ , with  $\varphi$  under different cohesions and slope

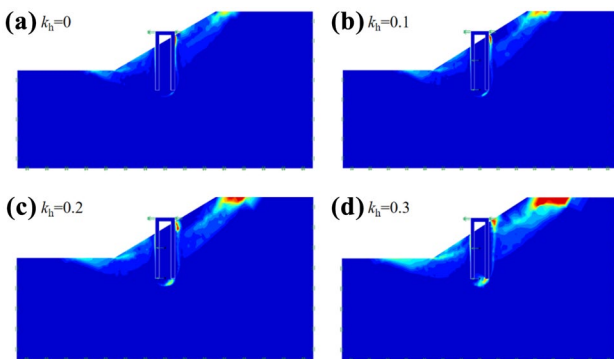
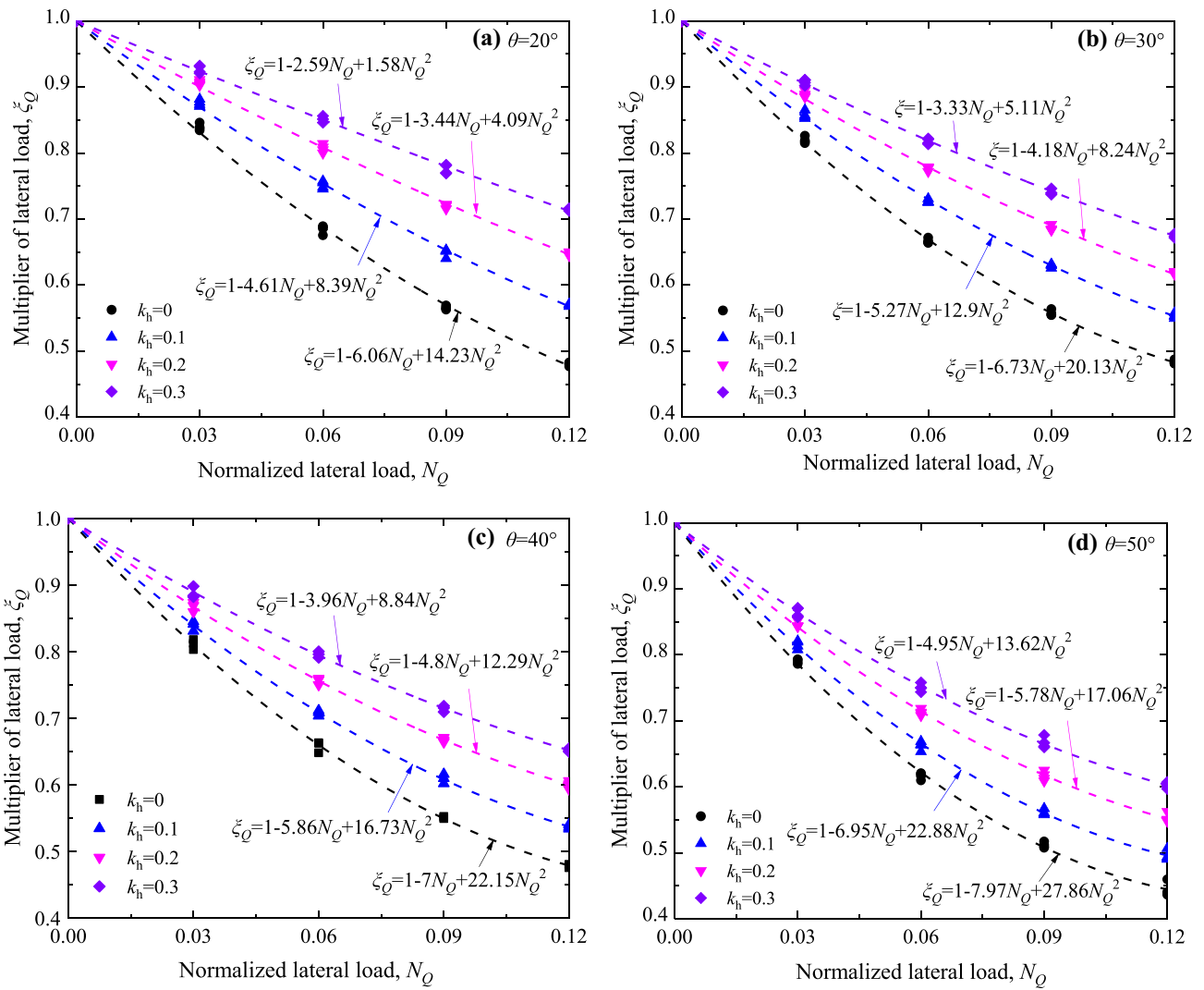


Fig. 7 Failure modes of slopes for  $\theta=30^\circ$ ,  $N_Q=0.06$ ,  $\varphi=25^\circ$ , and  $N_c=0.5$

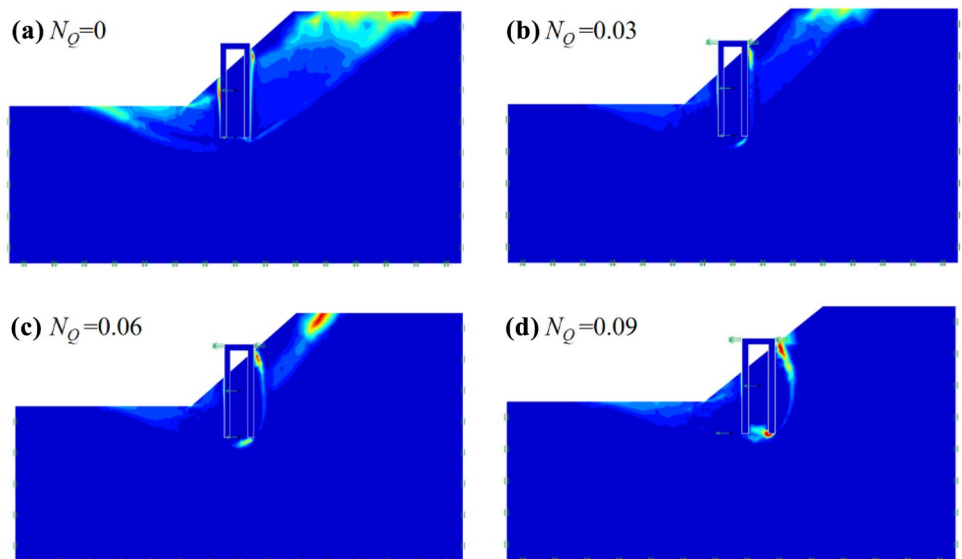
angles, and all groups of horizontal seismic coefficients and lateral loads are taken into consideration. The multiplier of internal friction angle linearly increases with  $\varphi$ , and so does the seismic safety factor of SCTPF. Furthermore, the variations of  $\xi_\varphi$  with  $\varphi$  can be fitted by linear functions,  $\xi_\varphi = B_\varphi \cdot (\varphi - 15^\circ) + 1$  (Fig. 12), and the fitting coefficients  $B_\varphi$  decrease with  $N_c$  and vary slightly with  $\theta$ . In addition, if other factors are kept the same, the multiplier of internal friction angle is insensitive to  $k_h$  and  $N_Q$ . To sum up, the effect of internal friction angle on the slope seismic stability would be independent of horizontal seismic coefficient, lateral load, and slope angle.

Figure 13 draws the variations of the multiplier of cohesion,  $\xi_c$ , with  $N_c$  under different internal friction angles and slope angles, and all groups of horizontal seismic coefficients and lateral loads are taken into consideration. The multiplier of cohesion increases with  $c$ , and so does the



**Fig. 8** Variations of  $\xi_Q$  under different horizontal seismic coefficients

**Fig. 9** Failure modes of slopes for  $\theta=40^\circ$ ,  $k_h=0.2$ ,  $\varphi=25^\circ$ , and  $N_c=0.5$



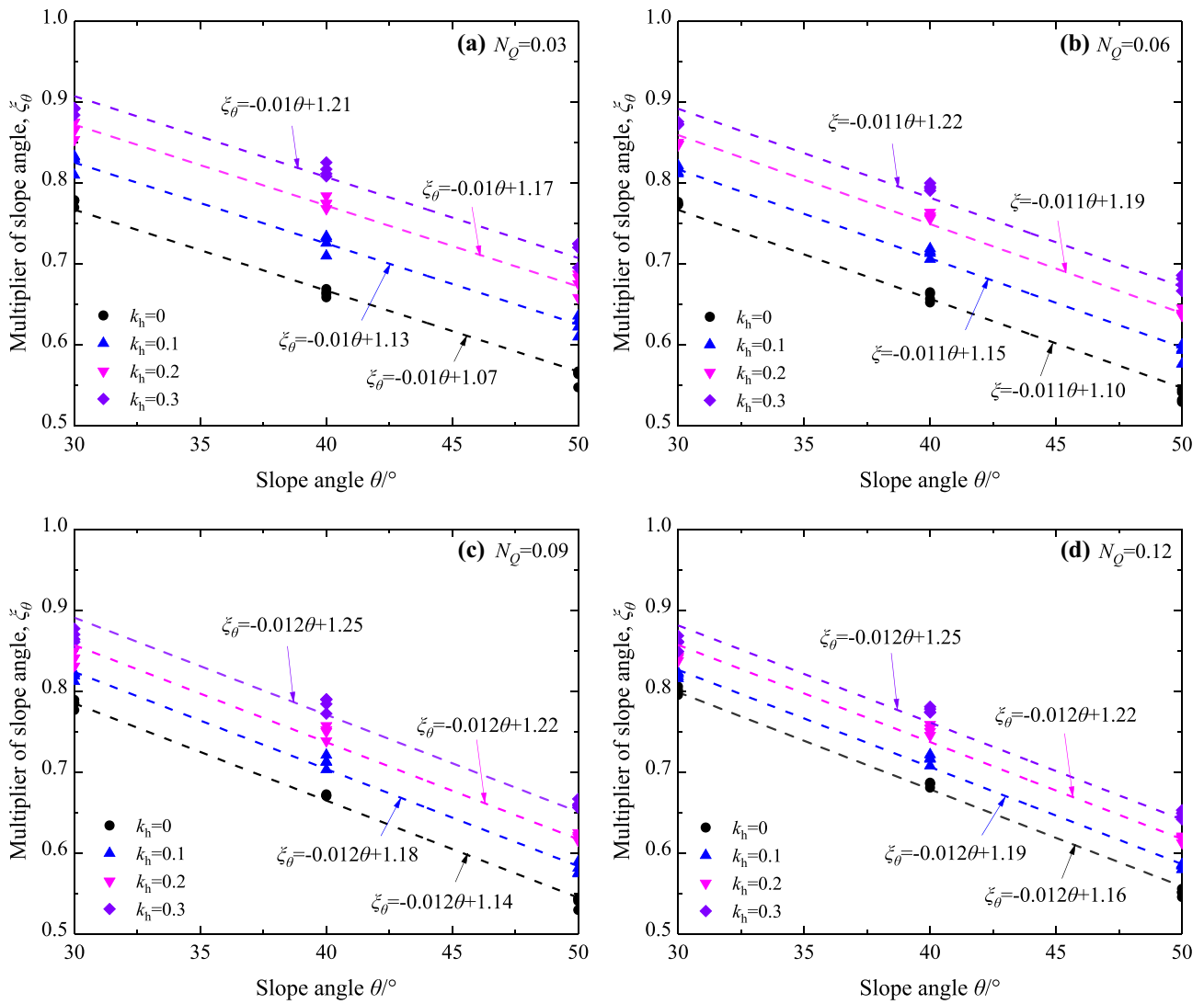
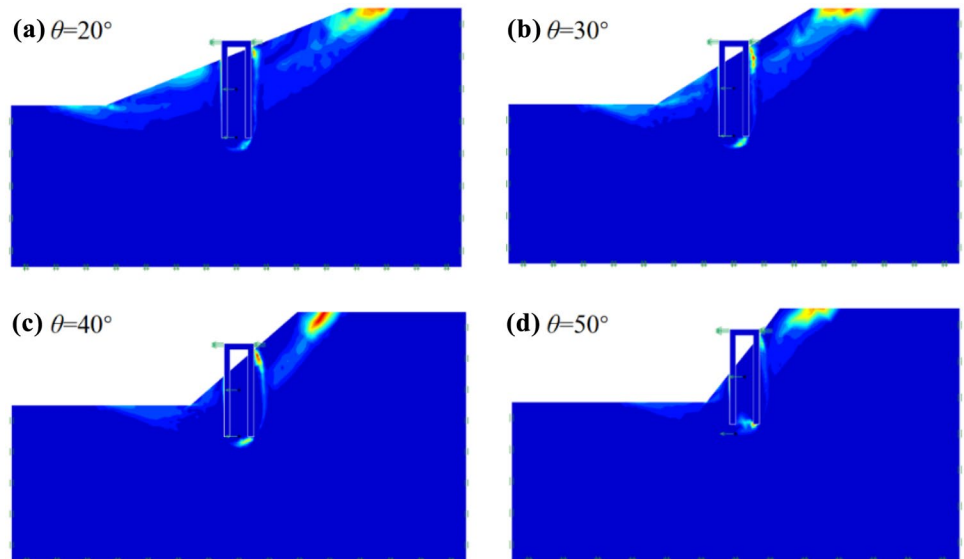
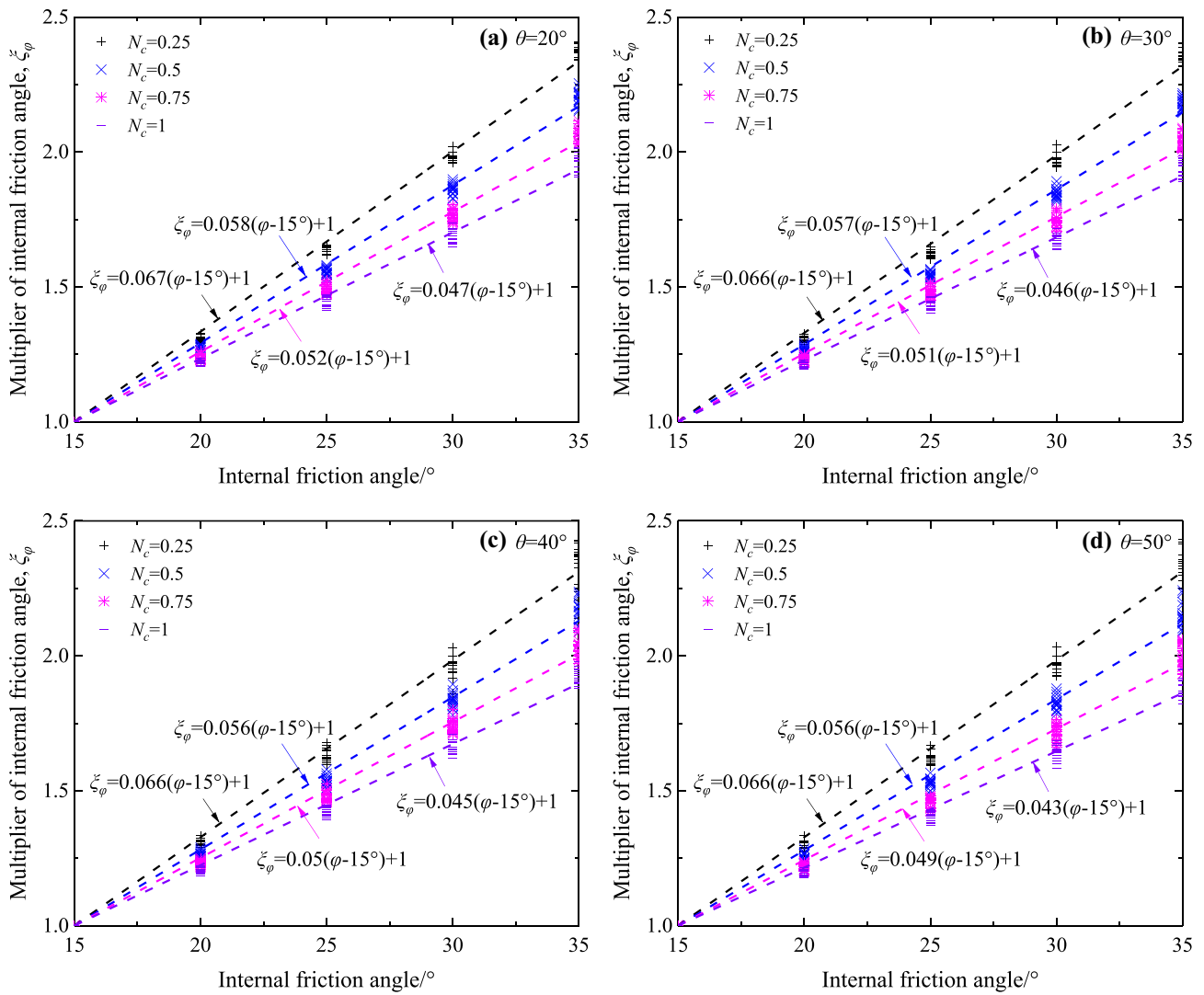


Fig. 10 Variations of  $\xi_\theta$  under different horizontal seismic coefficients

Fig. 11 Failure modes of slopes for  $N_Q=0.06$ ,  $k_h=0.2$ ,  $\varphi=25^\circ$ , and  $N_c=0.5$





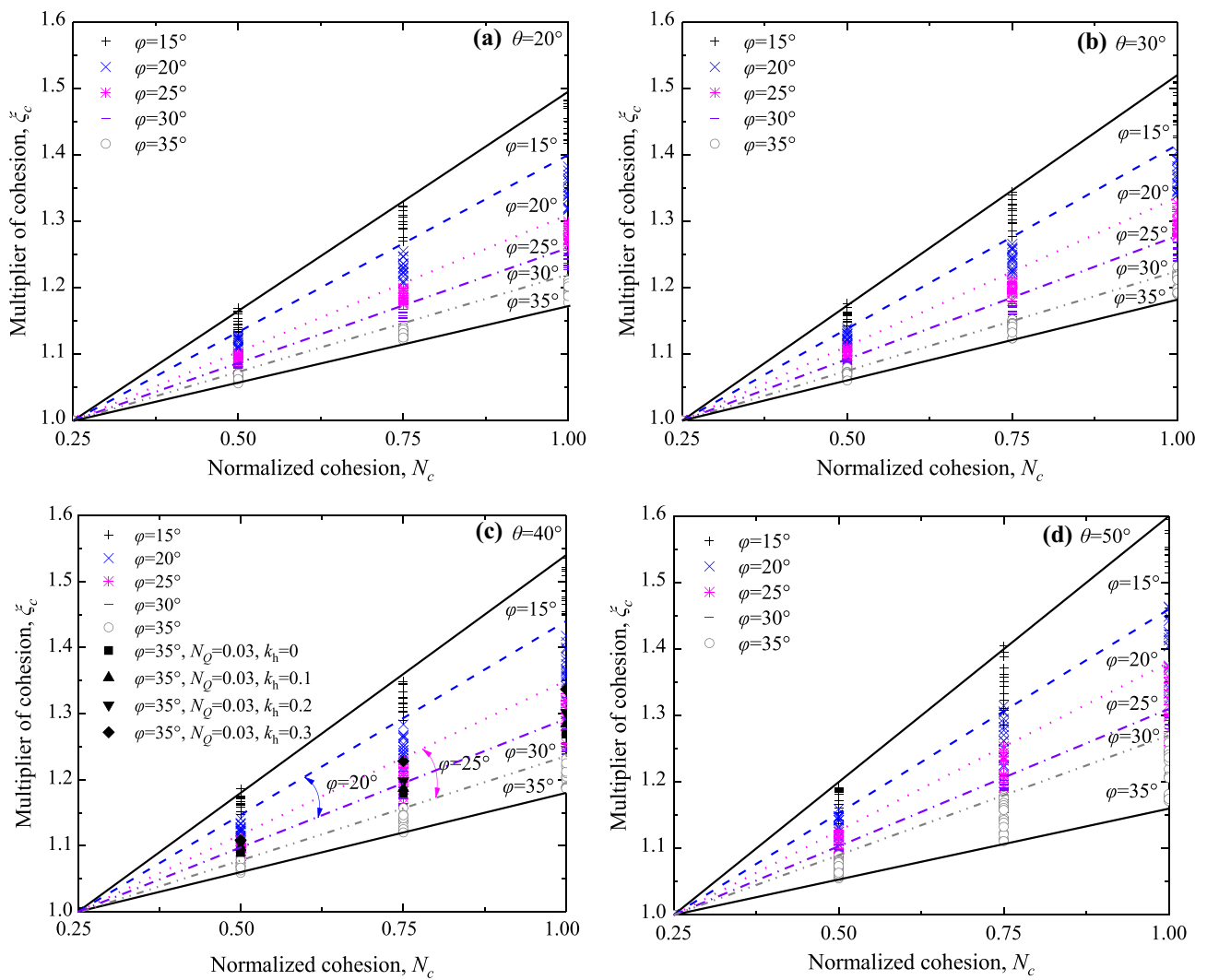


**Fig. 12** Variations of  $\xi_\phi$  under different cohesions

seismic safety factor of SCTPF. However, the multiplier of cohesion under different horizontal seismic coefficients and lateral loads is more discretely distributed than the multiplier of internal friction angle, and its variation with  $N_c$  cannot be well fitted by linear functions. The plotted area can be divided into clockwise rotating regions with  $\phi$  as per the internal friction angle, and the clear region boundaries indicate that the multiplier of cohesion mainly depends on  $\phi$  for most cases. However, there are some overlapped areas for the cases of  $\theta=40^\circ$  because the effects of internal friction angle, horizontal seismic coefficient, and lateral load are almost equal for the cases of  $\theta=40^\circ$ . The reason for the four groups of unexpectedly distributed points marked in Fig. 13c is the failure modes of the cases ( $N_Q=0.03$ ) are different from those of the cases ( $N_Q=0.06, 0.09, \text{ and } 0.12$ ) when

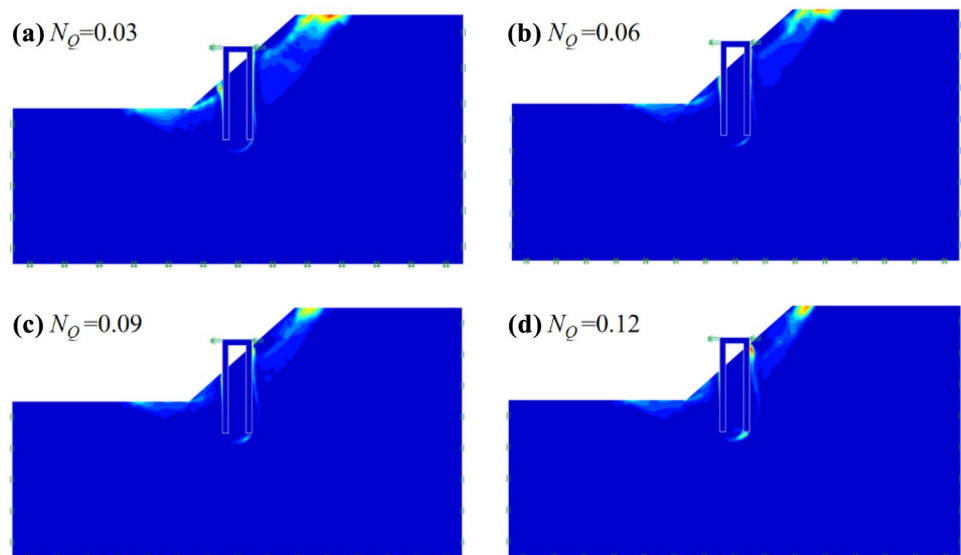
other factors are kept the same; a wedge failure would occur in the front of the pile foundation for the cases of  $N_Q=0.03$ , while the shear failure and tension failure are observed in the cases of  $N_Q=0.06, 0.09, \text{ and } 0.12$  as illustrated in Figs. 14 and 15.

Figure 16 demonstrates the plastic multipliers of an example SCTPF ( $\theta=40^\circ, N_Q=0.06, k_h=0.2$ ) under different shear strengths ( $\phi=20^\circ, N_c=0.25; \phi=25^\circ, N_c=0.5; \phi=30^\circ, N_c=0.75; \text{ and } \phi=35^\circ, N_c=1$ ). The failure modes of low shear strength case ( $\phi=20^\circ, N_c=0.25$ ) are distinctively different from those of high shear strength cases ( $\phi=25^\circ, N_c=0.5; \phi=30^\circ, N_c=0.75; \text{ and } \phi=35^\circ, N_c=1$ ). The failure mode would change from shallow sliding to shear sliding with increasing shear strength, and the transitional sliding mode would occur in the case of  $\phi=20^\circ$  and  $N_c=0.25$ .

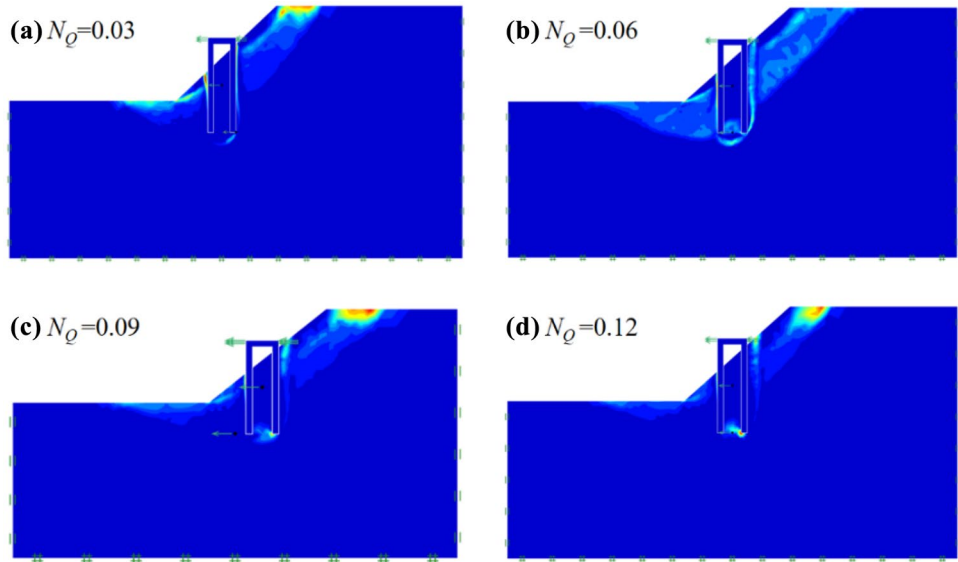


**Fig. 13** Variations of  $\xi_c$  under different internal friction angles

**Fig. 14** Failure modes of slopes for  $\theta=40^\circ$ ,  $k_h=0$ ,  $\phi=35^\circ$ , and  $N_c=0.75$



**Fig. 15** Failure modes of slopes for  $\theta=40^\circ$ ,  $k_h=0.2$ ,  $\varphi=35^\circ$ , and  $N_c=0.75$



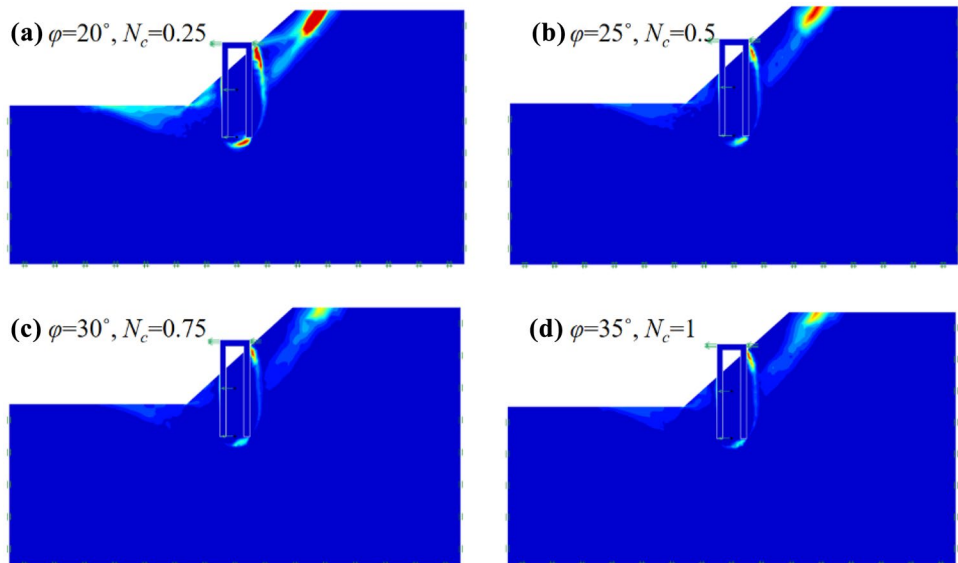
### Design tables and failure modes

Tables 5, 6, 7, and 8 list the predictions of static and seismic safety factors of SCTPF by FELA, and the failure modes can be approximately classified into six representative types according to these analyses:

- (a) Shallow sliding (Fig. 17a). It is frequently observed in the steep slope with low shear strength. The shear strength is too low to sustain the slope stability, and the potential failure surface would occur above the pile head.
- (b) Shear sliding (Fig. 17b). It is the most frequently encountered failure mode and has been referred to in the studies of the laterally loaded single pile in mountainous areas (Ng et al. 2001). Compared to the shallow sliding, the potential failure surface behind the pile foundation in this case would move down from the pile head to the upper section of the pile.

- (c) Transitional sliding (Fig. 17c). It is a transitional state between shallow sliding and shear sliding. The shear strength in this failure mode is greater than that in shallow sliding and less than that in shear sliding.
- (d) Wedge failure (Fig. 17d). It is a special case of shear sliding, and a wedge failure region can be observed in front of pile foundations in the cases of  $N_Q=0.03$ .
- (e) Deep shear sliding (Fig. 18). It is frequently encountered in the cases of low horizontal seismic coefficient and low lateral load. While the shear strength increases, the failure surface of the shear sliding behind the pile foundation would move down from the upper section

**Fig. 16** Failure modes of slopes for  $\theta=40^\circ$ ,  $N_Q=0.06$ , and  $k_h=0.2$



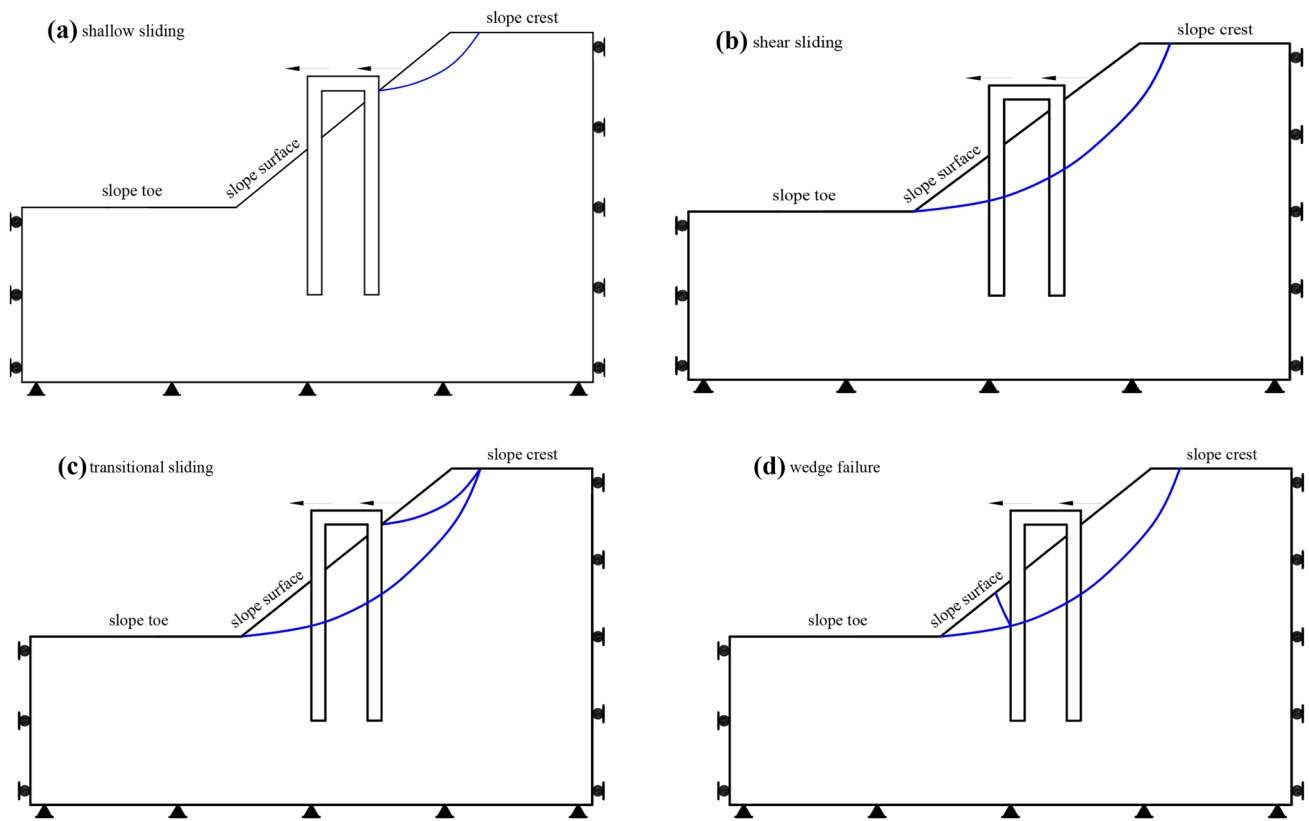


Fig. 17 Representative failure modes of SCTPF under seismic loads

of the pile to the pile tip (from the failure surface in Fig. 17b to that in Fig. 18a or b). The failure surface would be affected near the tip of the two-pile foundation and can be further divided into two subcategories I and II; the failure surface penetrates the pile above the pile tips, the failure surface between the piles will concave downward; however, the failure surface between the piles will concave upward when the failure surface further moves beneath the piles.

(f) Tension failure (Fig. 19). It usually appears in cases of great horizontal seismic coefficient and lateral load. The reason is that the slope is relatively stable only leaving the separation of the pile foundation from the rear soil, and the failure mode is significantly different from that of the anti-slide pile-reinforced slope. According to the soil deformation behind the pile, the failure mode can be further divided into two subcategories I and II: the tensioned crack occurs just adjoining

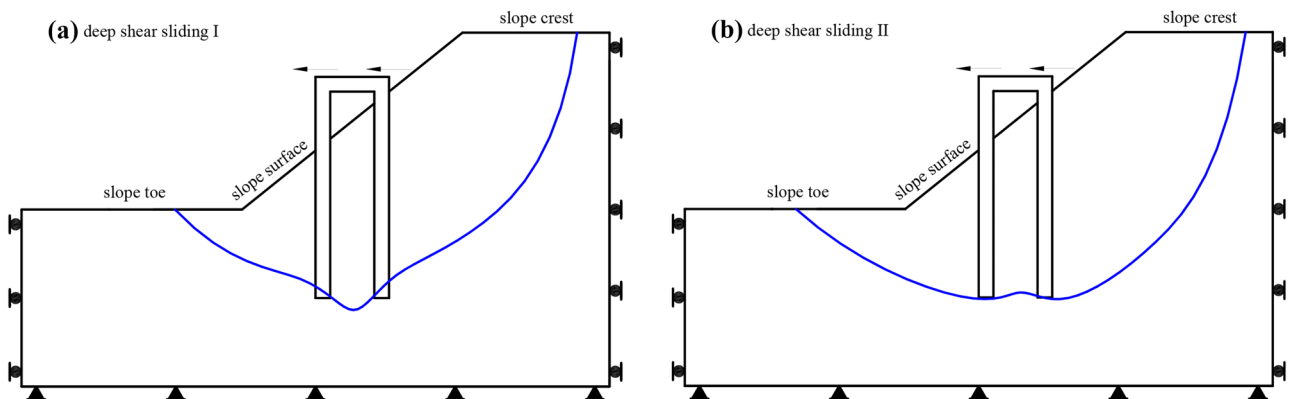


Fig. 18 Representative failure modes of SCTPF under seismic loads

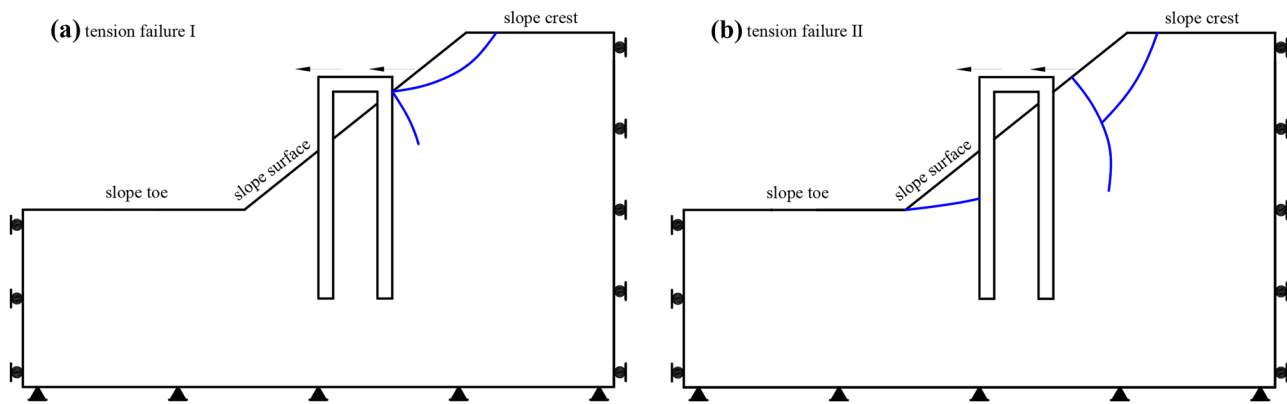


Fig. 19 Representative failure modes of SCTPF under seismic loads

the pile and the upper slip surface penetrates the slope with lower shear strength, horizontal seismic coefficient, and lateral load in the subcategory I; the tensioned crack will move away from the pile towards the slope crest, and it prevents the upper slip surface from penetrating the slope with increasing shear strength, horizontal seismic coefficient, and lateral load in subcategory II.

## Conclusions

This study concentrates on the effects of various factors ( $k_h$ ,  $N_Q$ ,  $\theta$ ,  $\varphi$ , and  $N_c$ ) on the seismic safety factor of SCTPF by FELA and presents some non-dimensional multipliers for general application. In addition, four detailed design tables and six representative failure modes have been summarized. Based on these analyses, several conclusions are drawn as follows:

- (i) The factors of safety of some slopes evaluated by FELA are in good agreement with those obtained from the limit equilibrium method, limit analysis method, and finite difference method, and the FELA method is proved to well evaluate the seismic stability of SCTPF.
- (ii) Some non-dimensional multipliers are presented to investigate the variations of seismic safety factors with different factors and simplify the calculation of seismic safety factors. For example, the seismic safety factor under seismic loads,  $FoS(k_h)$ , is the product of the safety factor,  $FoS(k_h=0)$ , and the corresponding multiplier of the seismic coefficient,  $\xi_k$ . On this basis, numerous values of the multipliers under different conditions have been given in this study and the tendency of these multipliers with different factors ( $k_h$ ,  $N_Q$ ,  $\theta$ ,  $\varphi$ , and  $N_c$ ) has been explored by fitting curves or distribution regions. The multiplier of horizontal seismic coefficient, the multiplier

of lateral load, and the multiplier of slope angle are not sensitive to shear strength.

- (iii) Many design tables for the safety factors of SCTPF under seismic loads are listed based on the predictions from FELA, covering most engineering cases. The tables are helpful to the preliminary design of similar projects and handy to engineers because the seismic safety factor of slopes can be directly looked up with precise values or approximately obtained by linear or nonlinear interpolation.
- (iv) The failure modes of SCTPF can be approximately classified into six representative failure modes: (a) shallow sliding; (b) shear sliding; (c) transitional sliding; (d) wedge failure; (e) deep shear sliding; and (f) tension failure. Furthermore, the mechanisms and conditions of these failure modes and the transitions among them are elaborated.

**Acknowledgements** The authors are thankful to OptumCE for the free access of OptumG2 program (academic edition) to perform this study.

**Funding** This research is part of work supported by grants from the National Natural Science Foundation of China (Nos. 52108317, 51978255, and 51908208) and the Hunan Provincial Natural Science Foundation of China (No. 2022JJ40074).

**Data availability** Some or all data, models, or codes that support the findings of this study are available from the corresponding author upon reasonable request (the data in the graph and the code of calculation, etc.).

## References

- Ausilio E, Conte E, Dente G (2001) Stability analysis of slopes reinforced with piles. *Comput Geotech* 28(8):591–611
- British Standards Institution (BSI) (1985) Structural use of concrete. Part 1—code of practice for design and construction (BS 8110: part 1: 1985). British Standards Institution, London
- Cinicoglu O, Erkli A (2018) Seismic bearing capacity of surficial foundations on sloping cohesive ground. *Soil Dyn Earthq Eng* 111(8):53–64



- Dai GL, Salgado R, Gong WM, Zhang YB (2012) Load tests on full-scale bored pile groups. *Can Geotech J* 49(11):1293–1308
- Editorial Board of Geological Engineering Handbook (2018) Geological engineering handbook. China Architecture and Building Press, Beijing, China ((in Chinese))
- Gao YF, Zhu D, Zhang F, Lei GH, Qin H (2014) Stability analysis of three-dimensional slopes under water drawdown conditions. *Can Geotech J* 51(11):1355–1364
- GB/T (Chinese Standards) 2021 Standard for classification of engineering soils. 50145—2007. Nanjing Hydraulic Research Institute, Jiangsu, China (in Chinese)
- Hassiotis S, Chameau JL, Gunaratne M (1997) Design method for stabilization of slopes with piles. *J Geotech Geoenviron Eng* 123(4):314–323
- Huang Y, Xu X, Liu J, Mao W (2020) Centrifuge modeling of seismic response and failure mode of a slope reinforced by a pile-anchor structure. *Soil Dyn Earthq Eng* 131(4):106037
- Jiang C, Zhang Z, He J (2020) Nonlinear analysis of combined loaded rigid piles in cohesionless soil slope. *Comput Geotech* 117:103225
- Joorabchi AE, Liang RY, Li L, Liu H (2014) Yield acceleration and permanent displacement of a slope reinforced with a row of drilled shafts. *Soil Dyn Earthq Eng* 57(2):68–77
- JTG 3363—2019 (2020) [In Chinese.] Specifications for design of foundation of highway bridges and culverts. China Communications Press, Beijing
- Kumar J, Chakraborty D (2013) Seismic bearing capacity of foundations on cohesionless slopes. *J Geotech Geoenviron Eng* 139(11):1986–1993
- Li X, Su L, He S, Xun J (2016) Limit equilibrium analysis of seismic stability of slopes reinforced with a row of piles. *Int J Numer Anal Meth Geomech* 40(8):1241–1250
- Li XP, He S, Wu Y (2010) Seismic displacement of slopes reinforced with piles. *J Geotech Geoenviron Eng* 136(6):880–884. [https://doi.org/10.1061/\(ASCE\)GT.1943-5606.0000296](https://doi.org/10.1061/(ASCE)GT.1943-5606.0000296)
- Li XP, Pei X, Gutierrez M, He S (2012) Optimal location of piles in slope stabilization by limit analysis. *Acta Geotech* 7(3):253–259
- Liang FY, Chen HB, Chen SL (2012) Influences of axial load on the lateral response of single pile with integral equation method. *Int J Numer Anal Meth Geomech* 36(16):1831–1845
- Lin ML, Wang KL (2006) Seismic slope behavior in a large-scale shaking table model test. *Eng Geol* 86(2):118–133
- Liu XR, Kou MM, Feng H, Zhou Y (2018) Experimental and numerical studies on the deformation response and retaining mechanism of h-type anti-sliding piles in clay landslide. *Environ Earth Sci* 77(5):1–14
- Liyanapathirana DS, Poulos HG (2010) Analysis of pile behaviour in liquefying sloping ground. *Comput Geotech* 37(1–2):115–124
- Loukidis D, Bandina P, Salgado R (2003) Stability of seismically loaded slopes using limit analysis. *Geotechnique* 53(5):463–479
- Muthukkumaran K (2014) Effect of slope and loading direction on laterally loaded piles in cohesionless soil. *Int J Geomech* 14(1):1–7
- Nakasima E, Tabara K, Maeda Y (1985) Theory and design of foundations on slopes. *Doboku Gakkai Ronbunshu* 355:46–52
- Ng CWW, Zhang LM (2001) Three-dimensional analysis of performance of laterally loaded sleeved piles in sloping ground. *J Geotech Geoenviron Eng* 127(6):499–509
- Ng CWW, Zhang LM, Ho KK (2001) Influence of laterally loaded sleeved piles and pile groups on slope stability. *Can Geotech J* 38(3):553–566
- Ni PP, Mei GX, Zhao Y (2018) Influence of raised groundwater level on the stability of unsaturated soil slopes. *Int J Geomech* 18(12):04018168
- Nian TK, Jiang JC, Wang FW, Yang Q, Luan MT (2016) Seismic stability analysis of slope reinforced with a row of piles. *Soil Dyn Earthq Eng* 84(5):83–93
- Nian TK, Chen GQ, Luan MT, Yang Q, Zheng DF (2008) Limit analysis of the stability of slopes reinforced with piles against landslide in nonhomogeneous and anisotropic soils. *Can Geotech J* 45(8):1092–1103
- Nimityongskul N, Kawamata Y, Rayamajhi D, Ashford SA (2018) Full-scale tests on effects of slope on lateral capacity of piles installed in cohesive soils. *J Geotech Geoenviron Eng* 144(1):04017103
- Optum Computational Engineering (2017) OptumG2: program for geotechnical finite element analysis. [www.optumce.com](http://www.optumce.com). Accessed 20 Mar 2021
- Peng WZ, Zhao MH, Zhao H, Yang CW (2020) A two-pile foundation model in sloping ground by finite beam element method. *Comput Geotech* 122(6):103503
- Peng WZ, Zhao MH, Zhao H, Yang CW (2021) Effect of slope on bearing capacity of laterally loaded pile based on asymmetric failure mode. *Comput Geotech* 140:104469
- Peng WZ, Zhao MH, Zhao H, Yang CW, Zhou S (2022a) Kinematic limit analysis of the slope encapsulating a laterally loaded pile. *Bull Eng Geol Env* 81(5):215
- Peng WZ, Zhao MH, Zhao H, Yang CW (2022b) Seismic stability of the slope containing a laterally loaded pile by finite element limit analysis. *Int J Geomech* 22(1):06021033
- Peng WZ, Zhao MH, Xiao Y, Yang CW, Zhao H (2019) Analysis of laterally loaded piles in sloping ground using a modified strain wedge model. *Comput Geotech* 107(3):163–175
- Poulos HG (1995) Design of reinforcing piles to increase slope stability. *Can Geotech J* 32:808–818
- Sloan SW (2013) Geotechnical stability analysis. *Geotechnique* 63(7):531–572
- Uto K, Maeda H, Yoshii Y, Takeuchi M, Kinoshita K, Koga A (1987) Horizontal behavior of pier foundations in a shearing type ground model. *Int J Rock Mech Min Sci Geomech Abstr* 24(3):113
- Wang L, Sun D, Yao Y, Wu L, Xu Y (2020) Kinematic limit analysis of three-dimensional unsaturated soil slopes reinforced with a row of piles. *Comput Geotech* 120(4):103428
- Xiao S, Zeng J, Yan Y (2017) A rational layout of double-row stabilizing piles for large-scale landslide control. *Bull Eng Geol Env* 76(1):309–321
- Yan K, He J, Cheng Q, Fan G, Wang Z, Zhang J (2020) A centrifugal experimental investigation on the seismic response of group-pile foundation in a slope with an inclined weak intercalated layer. *Soil Dyn Earthq Eng* 130(3):105961
- Zhang C, Jiang G, Lei D, Asghar A, Wang Z (2021) Large-scale shaking table test on seismic behaviour of anti-slide pile-reinforced bridge foundation and gravel landslide: a case study. *Bull Eng Geol Env* 80(6):1303–1316
- Zhang C, Jiang G, Su L, Lei D, Wang Z (2020) Large-scale shaking table model test on seismic performance of bridge-pile-foundation slope with anti-sliding piles: a case study. *Bull Eng Geol Env* 76(6):1429–1447
- Zhao B, Wang YS, Wang Y, Shen T, Zhai YC (2017) Retaining mechanism and structural characteristics of h type anti-slide pile (hTTP pile) and experience with its engineering application. *Eng Geol* 222:29–37

Springer Nature or its licensor (e.g. a society or other partner) holds exclusive rights to this article under a publishing agreement with the author(s) or other rightsholder(s); author self-archiving of the accepted manuscript version of this article is solely governed by the terms of such publishing agreement and applicable law.